Journal of Superconductivity, Vol. 12, No. 6, 1999

Radio Frequency-Single Electron Transistor: A Fast and Sensitive Electrometer Analogous to the Radio Frequency-Superconducting Quantum Interference Device

P. Wahlgren,[1] R. J. Schoelkopf,[2] A. A. Kozhevnikov,[2] P. Delsing,[1] D. E. Prober,[2] and T. Claeson[1]

Received 2 February 1999

We describe a new mode of operation of the single electron transistor (SET). The so-called RF-SET (radio frequency-SET) is a dual of the RF-SQUID (radio frequency-superconducting quantum interference device). It has been operated at frequencies above 100 MHz with a very high charge sensitivity ($1.2 \times 10^{-5} e/\sqrt{\text{Hz}}$). The large bandwidth, combined with a high sensitivity, will enable studies of the dynamics of mesoscopic systems on very short time scales.

KEY WORDS: Coupling circuit; radio frequency; RF-SQUID; single electronics.

The single electron transistor (SET) has outstanding charge sensitivity. Thus, it has been used as a sensor to study several systems characterized by small charge changes. The necessary high impedance of the SET [1] has resulted in a large RC time and limited its bandwidth to a few hundred hertz. By reducing the output capacitance [2] with the aid of a HEMT amplifier (preferably on the same chip), cutoff frequencies as high as 700 kHz have been achieved. We will describe a novel mode of operation, which we call RF-SET. It has improved the bandwidth of the SET to above 100 MHz.

The SET was proposed by Likharev and described as the dual of the DC-SQUID (direct current-superconducting quantum interference device) [3]. The SET consists of a small metallic island that is isolated from the electric environment by two small tunnel junctions. The total capacitance C_Σ of the island is small enough that the charging energy of a single electron, $E_C \equiv e^2/2C_\Sigma$ can prevent tunneling at voltages below a threshold value. The charge states of the island are discrete and equidistant in energy with the spacing E_C, but their positions can be continuously shifted by an externally induced charge. Thus, the SET can act as a transistor when these charging states are brought in and out of resonance with the Fermi levels of the two connecting electrodes. For a review, see [4].

The DC-SQUID is a superconducting ring interrupted by two Josephson junctions (weak links) that are very sensitive to magnetic field. An external flux causes a modulation of the discrete sequential tunneling of flux through the two junctions. In the SET, the threshold voltage is modulated by an externally induced charge. In the SQUID, the threshold current is modulated by an external magnetic flux. Hence, the two systems are the dual of one and the other; see Fig. 1. The duality transform reads [3]

$$Q \leftrightarrow \Phi$$

$$e \leftrightarrow \Phi_0$$

$$V \leftrightarrow I$$

$$C \leftrightarrow L$$

$$R \leftrightarrow G$$

$$\text{series connection} \leftrightarrow \text{parallel connection}$$

---

[1] Physics and Engineering Physics, Chalmers University of Technology, S-412 96 Göteborg, Sweden.

[2] Departments of Applied Physics and Physics, Yale University, New Haven, Connecticut 06520-8284.

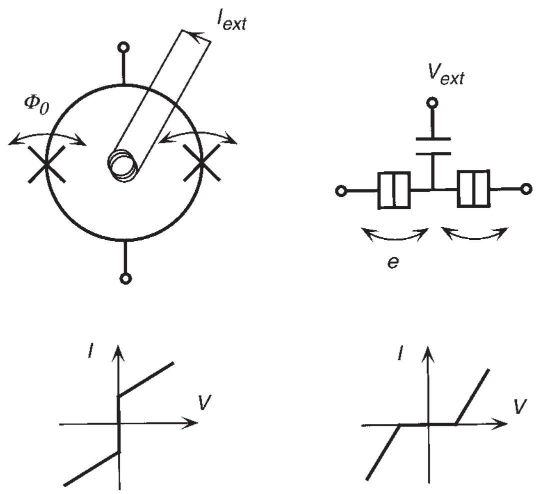

Fig. 1. The SET is, in many respects, the dual of the DC-SQUID. The onset of current corresponds to sequential tunneling events of electrons in the SET, while a voltage in the DC-SQUID is the result of periodic tunneling of magnetic flux quanta.

After the realization of the first SETs [5], an obvious question was if there were a useful dual circuit of the commonly used RF-SQUID (radio frequency-SQUID) [6]. The RF-SQUID consists of a single junction in a superconducting loop that is inductively coupled to a tank circuit driven at resonance (Fig. 2a) [7]. The dual circuit (see Fig. 2b) dissipates very small power unless operated with a tank circuit frequency close to the intrinsic 1/2 πRC frequency (where C is the capacitance and R is the resistance of the tunnel junctions). It can be chosen as high as 100 GHz.

A more attractive solution is to connect the island through a second tunnel junction. This RF-SET (radio frequency single electron transistor) configuration allows many tunnel events per cycle of the tank circuit oscillation, thus increasing the dissipated power in the tank circuit. The layout is similar (under the duality transformation) to a recently proposed type of SQUID, the double SQUID (D-SQUID [8]).

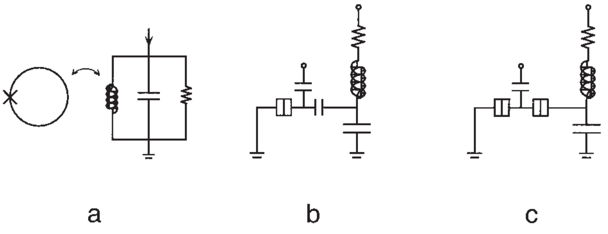

Fig. 2. (a) The RF-SQUID consists of a single Josephson junction loop inductively coupled to a tank circuit. (b) The dual of the RF-SQUID is a metallic island with one tunnel junction capacitively coupled to a tank circuit. (c) The RF-SET: an island with two tunnel junctions. The additional junction connects the island to the tank circuit.

1. EXPERIMENTS

The SET itself was a typical Al-based SET, fabricated using electron-beam lithography, a suspended resist bridge, and a double-angle evaporation technique [9]. The SET had $E_C/k_B = 2.1$ K. A schematic of our measurement setup is shown in Fig. 3. The source of the SET was grounded, and the connection to the drain was made by pressing a chip inductor, with an inductance of 27 nH, between a contact pad on the SET chip and the center pin of a 50-Ω semirigid coaxial cable. This cable connected the sample chip, cooled to 45 mK by the mixing chamber of a dilution refrigerator, to the main He bath, approximately 1 m away. The cable fed a 1.25–1.75 GHz HEMT-based low-noise amplifier, which had an input impedance of 50 Ω.

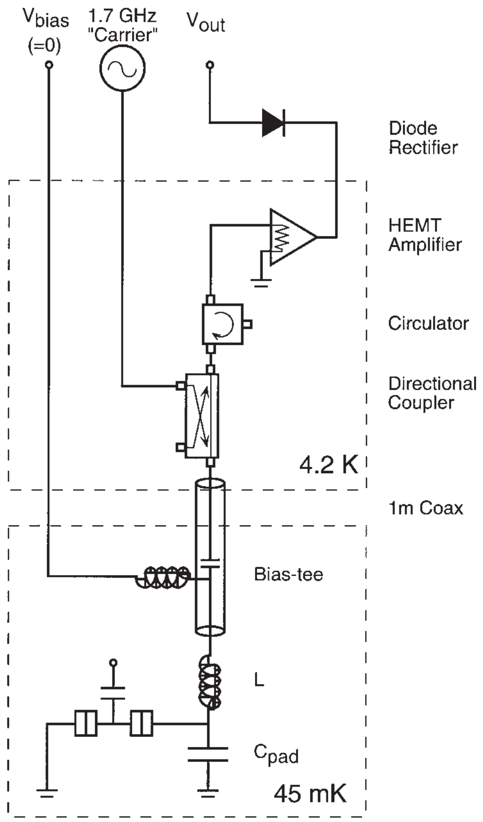

Fig. 3. The setup of the experiment.

The value of the series inductance was chosen so that it formed a resonant circuit together with the parasitic capacitance, $C_{\text{pad}} \approx 0.33$ pF, of the contact pad to the SET. The resonance frequency was about 1.7 GHz. A monochromatic signal at this resonance frequency, which we will refer to as the "carrier," was launched toward the SET and the reflected power was subsequently amplified and rectified. The variation in the reflected carrier power, as a function of the gate voltage, is shown in Fig. 4b for a small 1.7-GHz signal. The transistor's DC drain to source bias was zero, except for a small audio frequency signal, which was introduced via the bias tee and used to monitor the DC drain–source conductance.

2. RESULTS

The *I–V* characteristic of the SET is shown in Fig. 4a. The DC conductance displayed the familiar Coulomb blockade oscillations, with sharp conductance peaks separated by uniform intervals in gate voltage, corresponding to the addition of individual electrons to the transistor intermediate island, $\delta V_g = e/C_g$. It is apparent from Fig. 4 that the reflected carrier power is strongly correlated with the conductance of the transistor. When the conductance is a minimum, i.e., the transistor is in its blockade state, the reflected power is high, as would be expected for a transmission line terminated by an open circuit. On the other hand, when the transistor becomes conducting, some fraction of the carrier power is dissipated in the SET, and the reflected power decreases.

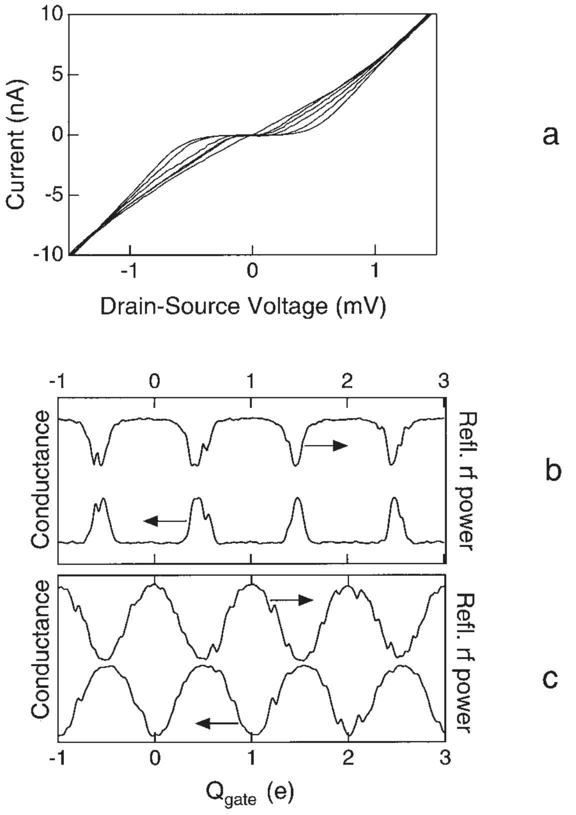

Fig. 4. (a) *I–V* characteristics of the SET measured at several different gate charges. (b) Conductance and reflected power versus induced charge ($Q_{\text{gate}} = C_{\text{gate}}V_{\text{gate}}$). (c) Conductance and reflected power at optimum carrier power.

The relative change is the reflected carrier power is small, because even the minimum resistance of the transistor is large compared to the characteristic impedance of the microwave system. Without the resonant circuit (C_{pad} and L), the expected fractional change in reflection [10] would be $\approx 4Z_0/R_{\min} \approx 10^{-3}$, where $R_{\min}$ is the resistance of the SET at one of the conductance maxima (see Fig. 4a), and $Z_0 = 50\ \Omega$ is the impedance of the cable and the amplifier. The inductor and the capacitor form a resonator and transform the impedance Z_0 upward at resonance. Thereby, the change in carrier reflection increases by a factor of Q^2, where Q is the quality factor of the resonator, $Q = \omega L/Z_0$. The measured "depth of modulation" for this device was 4%, in good agreement with the expected value $D = 4Q^2Z_0/R_{\min} \approx 3.7\%$, given the value of $Q \approx 6$.

For best sensitivity, the RF-SET was held at zero drain–source DC bias, and an AC voltage amplitude approximately equal to the threshold voltage (≈ 0.3 mV) was used. The DC conductance and the reflected carrier power under these conditions are shown in Fig. 4c. The large AC amplitude smooths out the conductance oscillations into an approximately sinusoidal form by sampling a wider range of drain–source bias voltage, but the fractional variation of the reflection remains unchanged. Note that the transfer function for the reflected power versus gate charge (or gate voltage, $V_g = Q_g/C_g$) is very similar to the curves of DC voltage versus gate charge for the usual type of SET when it is current-biased near threshold.

Both the microwave amplifier and the rectifying diode have bandwidths greater than 100 MHz. The impedance of the SET should respond to changes of the gate charge at even faster time scales, with a bandwidth of order $1/2\pi R_J C_J \approx 10$ GHz. The response of the RF-SET is shown in the time domain in Fig. 5a. A triangular wave ($\Delta Q = C_g V_g \approx 5.5e$ peak-to-peak) was applied to the gate. The data rep-

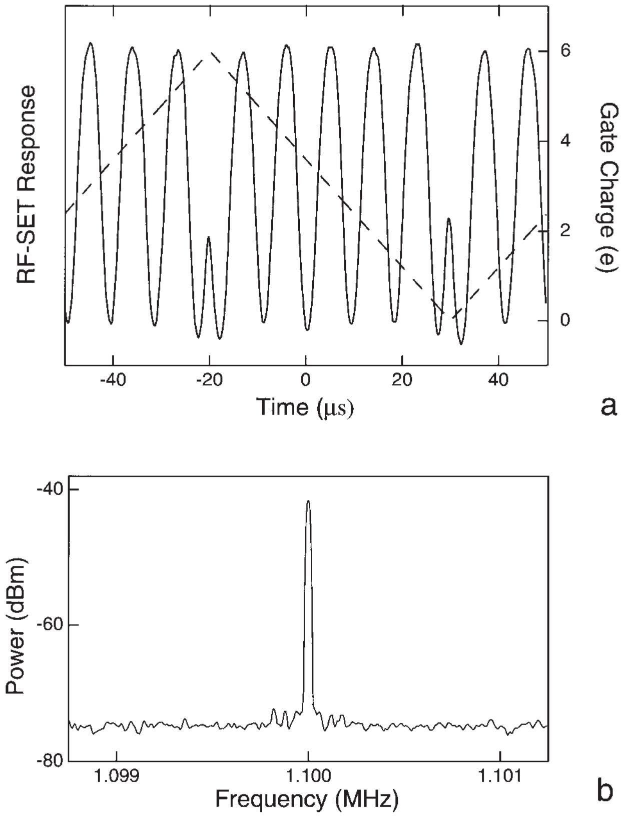

Fig. 5. Frequency response of the RF-SET. (a) Time-domain response of the RF-SET for a large ($\approx 5.5e$ p-p) signal, 10-kHz triangular wave (dotted line) applied to the gate. (b) Small-signal ($0.01e$ RMS) response for a 1.1-MHz sine wave on gate.

resent an average of 2,048 individual traces recorded on a digitizing oscilloscope. For each period of the triangular wave, the time average of the induced charge is changed by five electrons and back.

The device can also be used as a linear amplifier for small signals with a charge less than $|e|$, when the gate is DC-biased at a charge corresponding to the maximum slope of the sinusoidal response. The gate signal then causes an amplitude modulation of the carrier. At large gate signal frequencies, it is convenient to use an RF spectrum analyzer to detect the modulation at the output. Such a spectrum, showing the response to a small ($0.01e$ RMS) sinusoidal signal at 1.1 MHz, is shown in Fig. 5b. The gain displays the expected dependence of a DC potential on the gate, going to zero when the reflected power was at an extremum.

The very wide bandwidth of the RF-SET electrometer is illustrated in Fig. 6. The small-signal gain (obtained using a $\approx 0.01e$ RMS sine wave on the gate), varies less than 2 dB from 100 Hz to more than 40 MHz. Losses in the gate cable in the cryostat were signficant above 10 MHz and a gain correction had to be performed. Above 40 MHz, the gate was nearly opaque except for a narrow range close to 137 MHz. The gain obtained there (solid triangle in the diagram) is not significantly lower, indicating that the 3-dB gain bandwidth of this SET is in excess of 100 MHz.

The two bottom traces in Fig. 6 show the charge noise in units of $e/\sqrt{\text{Hz}}$. The two curves represent the SET in normal and superconducting (bottom) states. Above the $1/f$ corner (at about 3 kHz), the noise floor is set by the noise of the 1.7-GHz amplifier. The optimum value of the carrier power in the superconducting state was about 6 dB higher, as would be expected since the onset of current then occurs at $4\Delta/e + e/2C_\Sigma \approx 1$ mV. In addition, the current near the threshold and the dissipation in the RF-SET are more sharply peaked functions of the island charge in the superconducting state. This increases the SET gain and further reduces the white-noise contribution of the amplifier. We, therefore, observe an improved charge sensitivity in the superconducting state of $1.2 \times 10^{-5} e/\sqrt{\text{Hz}}$, which is a very competitive value, better than for any reported broad bandwidth electrometer [11]. The gain bandwidth in the superconducting case (not shown) was also larger than 50 MHz. In analogy with the practice used for low-noise SQUIDs, we can equate our charge noise to an effective energy sensitivity of the RF-SET, $\delta E = \delta q^2/2C_\Sigma = 4.3 \times 10^{-33}$ J/Hz, or $\approx 41\,\hbar$. Estimates show that the quantum limit $\approx 1\,\hbar$ should be obtainable for a device fabricated with the same technology as used here but with somewhat optimized parameters [12].

3. CONCLUSION

By coupling a radio frequency resonance circuit to a single electron transistor, it was possible to impedance-match the latter to the outside world and improve its frequency response and sensitivity at high frequency. Disregarding the $1/f$ noise at low frequency, it should be possible to approach a quantum limited noise operation as an electrometer. The function is dual to the one of an RF-SQUID where a low-impedance element is coupled to a tank circuit.

The RF-SET should be useful in many scientific applications thanks to the simultaneous achievement of high sensitivity and large bandwidth. It could provide the speed needed for current and capacitance

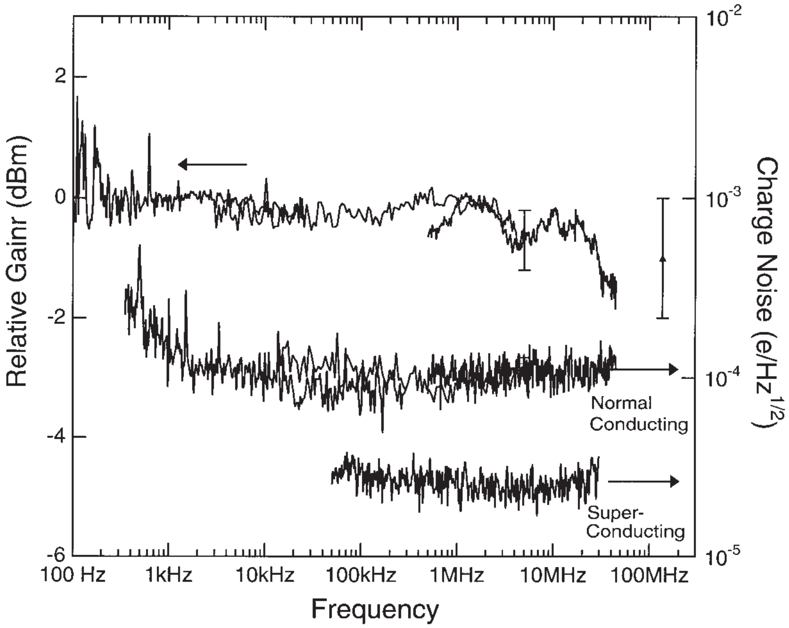

Fig. 6. Gain versus frequency for the RF-SET, showing the extremely large (≈100 MHz) bandwidth of the device. The frequency was limited mainly by cable losses in the cryostat, which cause the somewhat larger error bars at the highest frequency shown (137 MHz, solid triangle). The lower two traces show the system noise, expressed in $e/\sqrt{\text{HZ}}$, for operation in both normal and superconducting states.

standards [13]. It might also be fast enough to measure decoherence times in superconducting Cooper pair boxes, proposed as possible Q-bits in quantum computers [14]. The temperature of operation is still limited by the charging energy and our device degraded about 3 dB at 0.5 K. However, the RF-SET configuration can be used for devices in alternative techniques of fabrication or implementation. One improvement could be to use a superconductor with a large gap, suchas niobium [15]. The recent scanning SET microscope [16] could also benefit from a high-frequency mode of operation.

ACKNOWLEDGMENTS

This work was supported by the Swedish Natural Science and Technical Research Councils and the Wallenberg Foundation, as well as by U.S. National Science Foundation grants DMR-9216121 and AST-9320387. Samples were fabricated at the Swedish nanometer laboratory.

REFERENCES

1. The resistance of the tunnel junctions must be high $R_N \gg R_Q = h/4e^2$) so that charge fluctuations on the island will become negligible.
2. E. H. Visscher, J. Lindeman, S. M. Verbrugh, P. Hadley, J. E. Mooij, and W. van der Vleuten, *Appl. Phys. Lett.* **68,** 2014 (1996); J. Pettersson, P. Wahlgren, P. Delsing, N. Rorsman, D. B. Haviland, H. Zirath, and T. Claeson, *Phys. Rev. B* **53,** R13272 (1996); B. Starmark, P. Delsing, D. B. Haviland, and T. Claeson, in *Proc. Int. Superconductor Electronics Conf. (ISEC-97),* H. Koch. ed. (PTB, Berlin, 1997), p. 391.
3. K. K. Likharev, *IEEE Trans. Magnetics* **MAG-23,** 1142 (1987).
4. H. Grabert and M. Devoret, eds., *Single Charge Tunneling, Coulomb Blockade Phenomena in Nanostructures* (Plenum, New York, 1992)
5. T. A. Fulton and G. J. Dolan, *Phys. Rev. Lett.* **59,** 109 (1987), L. S. Kuzmin and K. K. Likharev, *JETP Lett.* **45,** 495 (1987).
6. K. K. Likharev, *Dynamics of Josephson Junctions and Circuits* (Gordon & Breach, New York (1986); Per Davidsson, Ph.D. thesis, Department of Physics, Chalmers University of Technology (1994).
7. T. Ryhänen, H. Seppä, R. Ilmoniemi, and J. Knuutila, *J. Low. Temp. Phys.* **76,** 287 (1989).
8. G. S. Krivoy and H. Koch, *J. Appl. Phys.* **74,** 2925 (1993); G. S. Krivoy and V. A. Komashko, *Physica B* **165, 166,** 83 (1990).
9. G. J. Dolan, *Appl. Phys. Lett.* **31,** 337 (1977).
10. The voltage reflection coefficient is given by $(Z - Z_0)/(Z + Z_0)$. When $Z = R_T \gg Z_0$, the total reflected power is proportional to

$1 - 4\,Z_0/R_T$. We assume that the impedance of the transistor, R_T, is very large at maximum blockade.

11. A charge noise of $8 \times 10^{-6} e/\sqrt{\mathrm{Hz}}$ has recently been obtained with a transimpedance amplifier and an Al superconducting SET in a narrow band near 4 kHz (B. Starmark, private communication).
12. R. J. Schoelkopf, P. Wahlgren, A. A. Kozhevnikov, P. Delsing, and D. E. Prober, *Science* **280,** 1238 (1998).
13. K. K. Likharev, in *Granular Electronics,* NATO ASI Series B: Physics Vol. 251, D. Ferry, ed. (Plenum, New York, 1990); M. W. Keller, J. M. Martinis, N. M. Zimmerman, and A. H. Steinbach, *Appl. Phys. Lett.* **69,** 1804 (1996).
14. V. Bouchiat, Ph.D. thesis, University of Paris (1997).
15. Y. Harada, D. B. Haviland, P. Delsing, C. D. Chen, and T. Claeson, *Appl. Phys. Lett.* **65,** 636 (1994).
16. M. J. Yoo, T. A. Fulton, H. F. Hess, R. L. Willett, L. N. Dunkleberger, R. J. Chichester, L. N. Pfeiffer, and K. W. West, *Science* **276,** 579 (1997).